Excitatory interneurons dominate sensory processing in the spinal substantia gelatinosa of rat

Sónia F. A. Santos[1,2], Sandra Rebelo[2], Victor A. Derkach[3] and Boris V. Safronov[1,2]

[1]*Instituto de Biologia Molecular e Celular – IBMC, Universidade do Porto, Rua do Campo Alegre 823, 4150-180 Porto, Portugal*
[2]*Laboratório de Biologia Celular e Molecular, Faculdade de Medicina, Universidade do Porto, Alameda Professor Hernâni Monteiro, 4200-319 Porto, Portugal*
[3]*Vollum Institute, Oregon Health & Science University, 3181 SW Sam Jackson Park Road, Portland, OR 97239, USA*

Substantia gelatinosa (SG, lamina II) is a spinal cord region where most unmyelinated primary afferents terminate and the central nociceptive processing begins. It is formed by several distinct groups of interneurons whose functional properties and synaptic connections are poorly understood, in part, because recordings from synaptically coupled pairs of SG neurons are quite challenging due to a very low probability of finding connected cells. Here, we describe an efficient method for identifying synaptically coupled interneurons in rat spinal cord slices and characterizing their excitatory or inhibitory function. Using tight-seal whole-cell recordings and a cell-attached stimulation technique, we routinely tested about 1500 SG interneurons, classifying 102 of them as monosynaptically connected to neurons in lamina I–III. Surprisingly, the vast majority of SG interneurons ($n = 87$) were excitatory and glutamatergic, while only 15 neurons were inhibitory. According to their intrinsic firing properties, these 102 SG neurons were also classified as tonic ($n = 49$), adapting ($n = 17$) or delayed-firing neurons ($n = 36$). All but two tonic neurons and all adapting neurons were excitatory interneurons. Of 36 delayed-firing neurons, 23 were excitatory and 13 were inhibitory. We conclude that sensory integration in the intrinsic SG neuronal network is dominated by excitatory interneurons. Such organization of neuronal circuitries in the spinal SG can be important for nociceptive encoding.

(Received 21 December 2006; accepted after revision 28 February 2007; first published online 1 March 2007)
Corresponding authors B. V. Safronov: Instituto de Biologia Molecular e Celular-IBMC, Universidade do Porto, Rua do Campo Alegre 823, 4150-180 Porto, Portugal. Email: safronov@ibmc.up.pt
V. A. Derkach: Vollum Institute, Oregon Health & Science University, 3181 SW Sam Jackson Park Rd, Portland, OR 97239, USA. Email: derkachv@ohsu.edu

The spinal substantia gelatinosa (SG), a dorsal horn region where most fine-calibre C- and Aδ-fibres terminate (Rethelyi, 1977; LaMotte, 1977; Light & Perl, 1977; Sugiura et al. 1986), is a key element in the nociceptive processing system. Diverse sensory modalities are encoded in the SG by the types of terminating afferents, the firing properties of intrinsic SG neurons and their synaptic connectivity (Brown, 1981; Cervero, 1987; Willis & Coggeshall, 1991).

Several groups of SG neurons with distinct intrinsic firing properties were characterized by both sharp electrode (Yoshimura & Jessell, 1989; Thomson *et al.* 1989; Lopez-Garcia & King, 1994) and tight-seal recordings (Grudt & Perl, 2002; Ruscheweyh & Sandkuhler, 2002; Santos *et al.* 2004; Graham *et al.* 2004). SG neurons with distinct firing properties show type-specific morphological features and intralaminar distributions (Grudt & Perl, 2002; Melnick *et al.* 2004*a*,*b*; Santos *et al.* 2004), but little is known about their synaptic connections. This knowledge is, however, important because neuronal firing activity and the strength of its synapses are related. Indeed, activity-dependent modification of synaptic strength, or synaptic plasticity, is an essential property of neuronal networks (Malenka & Nicoll, 1999; Turrigiano & Nelson, 2004; Malenka & Bear, 2004; Lisman & Spruston, 2005) and plays a key role in nociceptive processing and chronic pain development (Woolf & Salter, 2000; Ji *et al.* 2003; Salter, 2005). Thus, the firing pattern of a neuron can critically determine the efficiency of its functional connections and ultimately its contribution to the network activity. Therefore, to better understand how nociceptive information is processed within the superficial dorsal horn, it is essential to study firing patterns of SG interneurons and their synaptic connections.

Such investigation relies on identifying pairs of monosynaptically coupled neurons. This is a difficult task, however, if a conventional double patch-clamp recording technique is used, since the probability of finding monosynaptically connected neurons in slices of the

 DOI: 10.1113/jphysiol.2006.126912

superficial dorsal horn is very low (Lu & Perl, 2003). Indeed, recent studies have provided the first insight into the neuronal architecture of SG network showing that SG neurons form specific excitatory and inhibitory circuitries in the SG as well as lamina I (Lu & Perl, 2003, 2005). However, the total number of recordings from pairs of SG neurons is quite limited as well as the knowledge on the network organization. Therefore, we implemented a novel approach for efficiently identifying monosynaptic connections and studied discharge properties of excitatory and inhibitory SG interneurons. This approach combines a tight-seal whole-cell recording from postsynaptic neuron with a specific cell-attached stimulation of presynaptic neuron. We focused on two critical and unknown aspects of SG network organization: (1) the functional balance between the excitatory and inhibitory modes of sensory processing, and (2) whether and how neuronal firing properties correlate with their synaptic connections. We have characterized synaptic connections for SG neurons with different firing patterns and found that signalling within the SG network is dominated by excitatory glutamatergic interneurons.

Methods

Tight-seal recordings were made using both 200 μm transverse and 300 μm parasagittal slices prepared from the lumbar enlargement of the spinal cord of 2- to 7-week-old rats (Bentley & Gent, 1994; Melnick *et al.* 2004*a*). The animals were killed in accordance with the national guidelines (Direcção Geral de Veterinária, Ministério da Agricultura). After the anaesthesia by intraperitoneal injection of sodium pentobarbital (30 mg kg^{-1}), the vertebral column was quickly cut out and immersed in ice-cold oxygenated artificial cerebrospinal fluid (ACSF). The 5–7 mm segment of the lumbar enlargement was dissected and the slices were prepared using the tissue slicer (Leica VT 1000S). The slices were then incubated for 40–60 min in ACSF at 33°C. The SG (lamina II) was identified in the dorsal horn as a translucent band of about 60 μm thickness in its intermediate region (see Fig. 6). The marginal 20 μm layer of the dorsal horn separating the SG from the white matter was considered as lamina I. Neurons were localized during recording according to a position of the pipette tip on the video image of a superficial dorsal horn.

ACSF contained (mM): NaCl 115, KCl 3, $CaCl_2$ 2, $MgCl_2$ 1, glucose 11, NaH_2PO_4 1, $NaHCO_3$ 25, and glucose 11 (pH 7.4 when bubbled with 95%/5% mixture of O_2/CO_2). $MgCl_2$ was excluded from the ACSF used for recordings to avoid a possible block of the NMDA receptor-gated postsynaptic currents at potentials close to the resting membrane potential. Standard pipette solution contained (mM): KCl 3, potassium gluconate 150.5, $MgCl_2$ 1, BAPTA 1 and Hepes 10 (pH 7.3 adjusted with KOH, final $[K^+]$ was 160.5 mM). The theoretical reversal potential for Cl^- (E_{Cl}) was −81 mV in all experiments. The pipettes used for perforated-patch recordings were filled with solution containing (mM): NaCl 5, potassium gluconate 145, Hepes 10, amphotericin B (final concentration 100 μg ml^{-1}, freshly prepared from a 60 mg ml^{-1} stock solution). All chemicals were purchased from Sigma.

Recording pipettes were pulled from thick-walled borosilicate glass tubes (Modulohm, Denmark), fire-polished, and had a resistance of 3–5 MΩ. The pipettes used for cell-attached stimulation were narrower than those for the tight-seal recordings and had a resistance of 13–27 MΩ when fire-polished and filled with ACSF. An EPC-10-Double amplifier (HEKA, Lambrecht, Germany) was used in all experiments. The voltage-follower circuitry of the amplifier was employed for the current-clamp measurements. The effective corner frequency of the low-pass filter in voltage-clamp mode was 3 kHz. The frequency of digitization was always 10 kHz. Offset potentials were compensated directly before formation of a seal. Liquid junction potentials were calculated and corrected for in all experiments. The series resistance, determined in the current-clamp mode from the instantaneous voltage change produced by a current step injection, did not exceed 14 MΩ (with an exception of one cell). The voltage error due to resistance in series did not exceed 2 mV in all current-clamp recordings and was below 3 mV in all but three voltage-clamp experiments. Input resistances (R_{IN}) of neurons were measured in both current-clamp (using a −10 pA hyperpolarizing current of 500 ms duration) and voltage-clamp modes (from a change in a leakage current at a 100 ms voltage step from −80 to −120 mV).

Recordings in perforated patch mode were made 20–30 min after establishing the gigaseal contact with the cell. This time period allowed amphotericin B to perforate the membrane under the pipette and reduce the access resistance. Stable recording with perforated patches lasted for up to 2 h. Stability of perforated patches was controlled by adding to the pipette solution fluorescent dye Alexa 694. Only when patch membrane had been ruptured did the cell body also become fluorescent.

Resting membrane potential (V_R) is critical for pattern identification in some types of SG neurons and therefore special precaution was taken to correctly estimate it. Since the R_{IN} in SG neurons is in the gigaohm range, an unbalanced steady-state current of just a few picoamps at the amplifier input could substantially influence the measured V_R value (Santos *et al.* 2004). Thus, we balanced the input of the amplifier in a current-clamp mode before each experiment using a 0.5 GΩ resistor model circuitry in accordance with a procedure described by Santos *et al.* (2004). The remaining uncompensated input current was less than 1 pA.

SG neurons were separated into three groups on the basis of their firing properties, tonic neurons (TNs), adapting neurons (ANs) and delayed-firing neurons (DNs) as described in detail by Santos *et al.* (2004). In brief, TNs were able to support tonic firing during 500 ms depolarization induced by a sustained current injection. They had a low mean firing threshold of about −50 mV and 10–20 pA current pulses were sufficient to evoke firing (Santos *et al.* 2004; Melnick *et al.* 2004*a*). Under voltage-clamp condition, TNs showed inward rectification. A characteristic feature of ANs was a burst-like firing of spikes only at the beginning of depolarization. The mean firing threshold of about −50 mV was not significantly different from that in TNs (Santos *et al.* 2004; Melnick *et al.* 2004*b*). In both TNs and ANs, a transient K^+ current was not seen at voltage steps from −80 to −60 mV (Melnick *et al.* 2004*a*,*b*). A principal difference of DNs was the presence of a large transient K^+ current that substantially influenced the firing pattern. The spike threshold in DNs (about −40 mV, Santos *et al.* 2004) was considerably higher than in TNs or ANs and was reached at stimulation as strong as 50–70 pA, since a large portion of injected current was compensated by activating the transient K^+ current. In DNs the first spikes typically appeared with a considerable time delay at the end of the pulse and moved to its beginning as the stimulation increased. An inward rectification was less pronounced in DNs. There were, however, some minor variations in discharge patterns of DNs at strong stimulation. Some cells discharged regularly during the whole pulse, while others belonging to this group showed either interrupted bursts or single spikes (Santos *et al.* 2004). In Table 3 these subtypes of DNs are called DN_1, DN_2 and DN_3, respectively.

All numbers are given as mean ± standard error of the mean (S.E.M.). The parameters were compared by independent Student's *t* test. The present study is based on recordings from 249 superficial dorsal horn neurons, 217 of which were located in the SG. These statistics do not include the cells from the control experiments, in which inhibitory interneurons were selectively searched, to avoid bias toward the contribution of inhibitory neurons. All experiments, except those in Fig. 2*B*, were carried out at room temperature of 22–24°C.

Results

Our experiments were designed to (1) find monosynaptically connected pairs of superficial dorsal horn neurons with a presynaptic neuron located in the SG, (2) identify excitatory or inhibitory nature of the synapse, (3) correctly record the intrinsic firing patterns of presynaptic neurons, and (4) map the network connections of SG neurons within the superficial dorsal horn.

Identification of monosynaptic connections

Throughout this study the action potentials in presynaptic neurons were evoked using a cell-attached stimulation, specific for stimulated cell. The efficiency of this technique was first tested by the simultaneous whole-cell current-clamp recording from extracellularly stimulated neuron (Fig. 1*A*, $n = 12$). A 1 ms current pulse of 100 nA was applied to a stimulation pipette at a frequency of 1 Hz as it was approaching the cell. The stimulation artifacts were clearly recorded by the whole-cell electrode but a membrane depolarization was very small. After the stimulation pipette has been brought in a contact with the membrane of the cell soma, the amplitude of the stimulation artifact recorded by the whole-cell electrode increased but the membrane depolarization was still insufficient to excite the cell. An application of a slight negative pressure to the stimulation electrode, which increased the seal resistance several times, resulted in a membrane depolarization sufficient for activation of a spike at each stimulation pulse. The overshoot of the extracellularly activated spike was similar to that of the first spike in a train evoked by direct injection of depolarizing current through the whole-cell electrode (Fig. 1*A*). If a stronger negative pressure was applied to the stimulation electrode, the overshoot potential in all cells increased to non-physiological values of more than +100 mV (not shown). When the contact between the membrane and the stimulation pipette had been broken, the neuron no longer responded to the extracellular stimulation, indicating that the stimulation was efficient only for the attached neuron. The stimulation technique was effective for all three types of neurons studied. One pipette could be repeatedly used to stimulate different cells, thus providing an efficient method for searching presynaptic neurons.

To identify SG neurons as excitatory or inhibitory interneurons, we used the experimental protocol shown in Fig. 1*B*. First, a postsynaptic neuron located in laminae I–III was voltage clamped at −80 mV. The extracellular pipette was then brought in contact with a SG neuron which was presumably presynaptic, and a slight negative pressure was applied. After this, a voltage command changed the membrane potential in the postsynaptic neuron for 100 ms to −100 and −60 mV before returning back to −80 mV. Thirty milliseconds after beginning of each voltage step, a 1 ms current pulse of 100 nA was applied through the cell-attached pipette to the presynaptic neuron. If the neurons were connected, synaptic responses were evoked in a postsynaptic neuron at three different potentials at a 10 Hz frequency (100 ms stimulation interval). The same voltage command was repeated three more times (without stimulating a presynaptic neuron) in order to obtain an averaged trace used for subtraction of transients, leakage currents

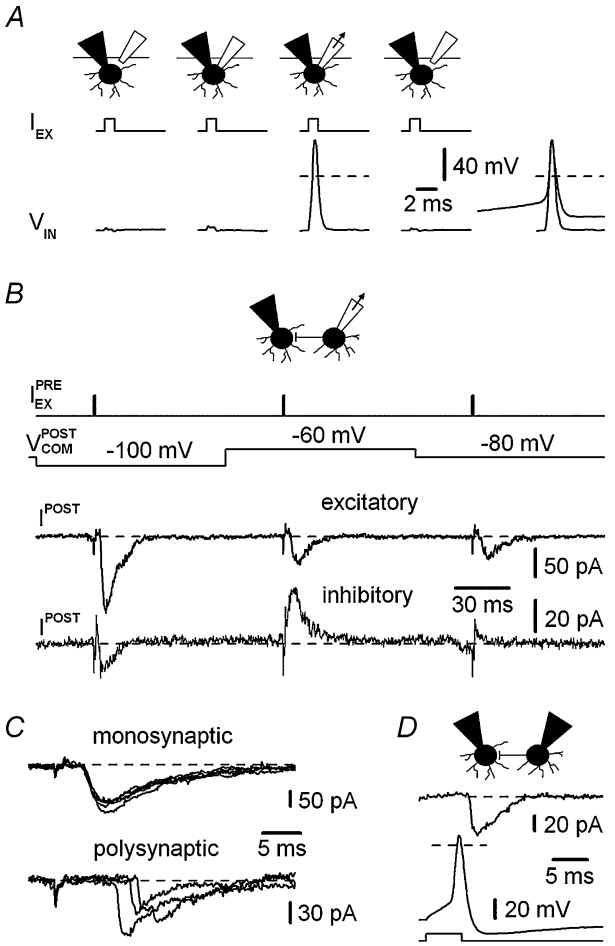

Figure 1. Focal cell-attached stimulation
A, in control experiments a direct whole-cell current-clamp recording from the extracellularly stimulated neuron was done. A 1 ms current pulse of 100 nA was injected through an artificial cerebrospinal fluid (ACSF)-filled stimulation pipette at a frequency of 1 Hz. Note the stimulation artifacts recorded intracellularly. Simple touching of the cell by the stimulation pipette (without pressure application) did not result in spike activation. However, spikes appeared at each current pulse after a slight negative pressure had been applied to the stimulation electrode and disappeared after an electrode had been withdrawn (with a positive pressure). The rightmost traces show superimposed the extra- and intracellularly (the first spike in a train) activated spikes. *B*, experimental procedure used for identifying the excitatory and inhibitory neurons. The postsynaptic currents (I_{POST}) were recorded in a voltage-clamped neuron at −100, −60 and −80 mV (each potential applied for 100 ms, $V_{COM,POST}$) while the presynaptic neuron was focally stimulated at 100 ms intervals (frequency of 10 Hz, $I_{EX,PRE}$). Recordings from two different neurons allowing characterization of their presynaptic connections as excitatory (upper) and inhibitory (lower). *C*, comparison of mono- and polysynaptic responses. Monosynaptic connection: first pulses (to −100 mV) from five consecutive voltage commands similar to those in part *B* are shown superimposed. The interval between voltage commands was 1.5 s. Polysynaptic connection: three non-consecutive pulses to −100 mV (empty episodes recorded in between are not shown). *D*, simultaneous whole-cell recordings from two synaptically connected neurons. An action potential activated by a direct injection of current pulse (100 pA, 5 ms) in a presynaptic neuron evoked a short latency inward current in a postsynaptic neuron voltage clamped at −80 mV.

and voltage-gated K^+ currents (activated at −60 mV). Thus, corrected traces shown in all figures contain only stimulation artifacts and postsynaptic currents. If the neurons appeared to be not connected, we progressively increased a negative pressure in the stimulation pipette to evoke large overshoot spikes in the presumably presynaptic neuron to ensure that lack of a postsynaptic response was not caused by insufficient stimulation of the presynaptic neuron.

A presynaptic neuron was considered as excitatory if its stimulation evoked inward postsynaptic currents at −100, −60 and −80 mV. A neuron was considered as inhibitory if the currents were inward at −100 mV and outward at −60 mV, becoming negligible at −80 mV, a potential close to an E_{Cl} of −81 mV. If the postsynaptic neuron was switched to current clamp, the corresponding excitatory or inhibitory postsynaptic potentials, EPSPs or IPSPs, were observed. This classification was also confirmed by specific receptor pharmacology: excitatory postsynaptic currents (EPSCs) were blocked by the AMPA/kainate receptor antagonist 6-cyano-7-nitroquinoxaline-2,3-dione (CNQX) (10 μM, $n = 16$), while inhibitory postsynaptic currents (IPSCs) were blocked by the glycine receptor antagonist strychnine (1 μM, $n = 6$). In eight early experiments, excitatory connections were identified on the basis of EPSPs recorded in a current-clamped postsynaptic neuron.

The responses were considered monosynaptic if they showed a constant latency and low percentage of failures at 10 Hz stimulation (Fig. 1*B*, three postsynaptic currents were recorded at different potentials with intervals of 100 ms). Figure 1*C* shows monosynaptic EPSCs recorded at first voltage steps to −100 mV from five consecutive voltage commands similar to those shown in Fig. 1*B*. In contrast, polysynaptic EPSCs could be clearly distinguished on the basis of variable latencies and frequent failures (Fig. 1*C*, failures are not shown). Polysynaptic connections were not included into this study.

The percentage of monosynaptically connected neurons in both parasagittal and transversal slices was low. A total of 173 connections (156 excitatory and 17 inhibitory) were found by testing about 1500 presumably presynaptic neurons. A tight-seal recording could be, however, established with 102 presynaptic neurons (87 excitatory and 15 inhibitory) that are described in this study. Recordings of postsynaptic currents and potentials, as well as blocker testing, were done using the cell-attached stimulation of a presynaptic neuron. At the end of the experiment we retained the stimulation pipette as a marker of the presynaptic neuron position, while the other pipette had been changed to establish a whole-cell mode and to record discharge pattern in the presynaptic neuron. In five control experiments, simultaneous whole-cell recordings from connected neurons were done (Fig. 1*D*). In this case, the recording from the postsynaptic neuron continued,

while a position and a shape of the presynaptic neuron was carefully marked on the video monitor and the stimulation pipette had been substituted with the second whole-cell electrode. In all five connections, an action potential elicited by a direct current injection to a presynaptic neuron was followed by the EPSCs in a postsynaptic one. The time delays and the kinetics of EPSCs were indistinguishable from those seen with the extracellular cell-attached stimulation.

Determination of firing patterns. We have previously characterized three types of SG neurons – TNs, ANs and DNs – on the basis of their firing patterns (Santos *et al.* 2004; Melnick *et al.* 2004*a*,*b*; see Methods). However, the reports on the discharge properties of SG neurons studied by the patch-clamp technique are controversial (Grudt & Perl, 2002; Lu & Perl, 2003; Hantman *et al.* 2004; but see Ruscheweyh & Sandkuhler, 2002). Differences in firing patterns reported in our studies and others may be a consequence of a number of experimental factors, such as measured mean values of V_R (varying from −48 to −77 mV) and R_{IN} (ranging from about 160 MΩ to 1.7 GΩ) or usage of different intracellular solutions. In addition, intrinsic discharge patterns might depend on whether the measurements are carried out at room temperature or at 37°C. Therefore, we first tested the firing patterns and measured V_R and R_{IN} in SG neurons using the least invasive form of the patch-clamp technique, perforated-patch recording (Horn & Marty, 1988; Rae *et al.* 1991), which prevents dialysis of cytoplasmic factors and alteration in divalent cation concentrations that normally occur in the whole-cell mode.

In experiments with perforated patches shown in Fig. 2*A* we recorded the same three basic types of SG neurons, TNs ($n = 10$), ANs ($n = 10$) and DNs ($n = 10$), as described by Santos *et al.* (2004). We found that the firing patterns were stable and could be recorded without modification for up to 2 h. The V_R values measured with a balanced amplifier input were close to −70 mV, and the mean R_{IN} obtained in current clamp was above 1 GΩ for all three types of neurons (Table 1). For five neurons of each type, the temperature of the solution was increased to 35–37°C (Fig. 2*B*). This did not modify the characteristic discharge pattern, implying that a correct identification of SG neuron could be done at room temperature.

In whole-cell recordings with our pipette solution (1 mM BAPTA) the same three types of SG neurons were seen. In test experiments with 15 neurons (five of each type) stable unmodified firing patterns were recorded during periods of 42 min to 2 h 1 min. Altogether, the whole-cell recordings were made from 186 SG neurons of which 89 were classified as TNs, 37 as ANs and 60 as DNs. The mean V_R and R_{IN} measured in whole-cell mode (see Table 1) were close to those of perforated-patch recordings. We thus concluded that the whole-cell recording with our internal solution was adequate for correctly characterizing pattern, V_R and R_{IN} in SG neurons.

Presynaptic TNs

Of the total 102 presynaptic SG neurons that were studied, 49 were identified as TNs (Fig. 3*A*). A majority of their synaptic connections (36 of 49; 73%) were intralaminar with another SG neurons, whereas only eight were found with lamina I, and five with lamina III neurons (Fig. 6*A* and Table 2). According to firing patterns, 31 of 49 connections were formed with TNs, 8 with ANs and 10 with DNs (Fig. 6*A* and Table 2). It should be noted that all postsynaptic neurons located in lamina I were TNs.

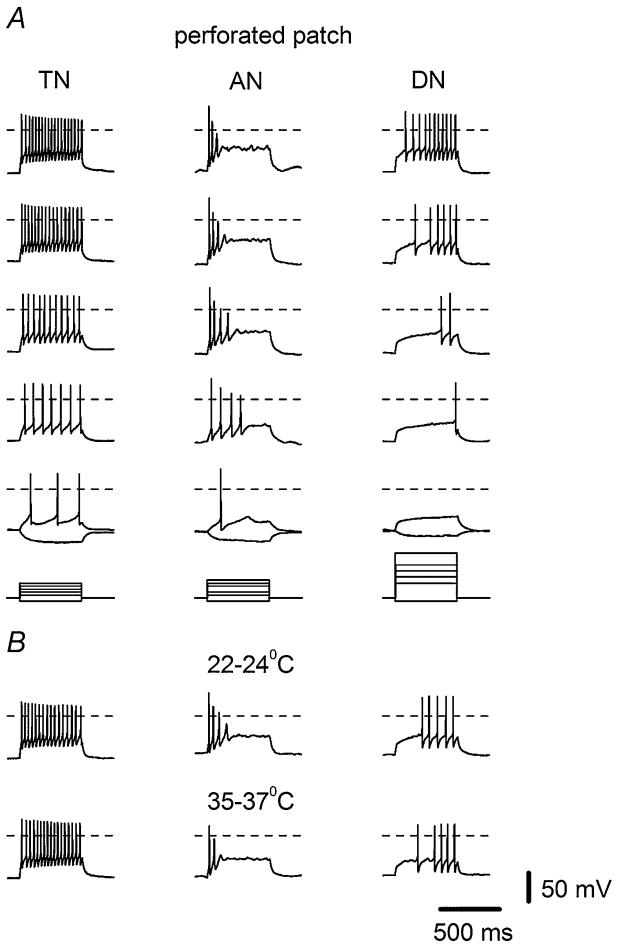

Figure 2. Perforated-patch recording of firing patterns of substantia gelatinosa (SG) neurons
A, membrane responses in a tonic neuron (TN), an adapting neuron (AN) and a delayed-firing neuron (DN) to 500 ms current injections. Stimulation protocols are shown below the traces. Passive membrane responses were elicited by an injection of a hyperpolarizing current of 10 pA (all depolarizing currents are appropriately scaled). *B*, discharge patterns of a TN, an AN and a DN at 22–24°C and 35–37°C. In all traces in this and the following figures dashed lines indicate 0 mV or 0 pA.

Table 1. The mean V_R and R_{IN} values measured in perforated-patch and whole-cell recordings

	R_{IN} (GΩ)		V_R (mV)	
	Whole cell	Perforated patch	Whole cell	Perforated patch
TN	2.26 ± 0.12 (89)	2.22 ± 0.48 (10)	−72.8 ± 0.4 (89)	−71.4 ± 0.5 (10)
AN	1.90 ± 0.18 (37)	2.02 ± 0.31 (10)	−71.8 ± 0.5 (37)	−70.3 ± 0.8 (10)
DN	1.69 ± 0.11 (60)	1.59 ± 0.37 (10)	−74.1 ± 0.4 (60)	−74.7 ± 0.7 (10)

R_{IN}, input resistance. The membrane potential (V_R) was measured with a balanced amplifier input (see Methods) in a total of 186 whole-cell modes and 30 perforated patches. Numbers of recordings are given in parentheses.

The distances between synaptically coupled neurons varied from 6 to 75 μm, with a mean distance of 19.2 ± 2.1 μm ($n = 49$).

All but two connections of TNs were excitatory. The mean maximum EPSC amplitude measured at −100 mV was 90.3 ± 10.6 pA ($n = 20$). The time course of decay was monoexponential with a mean time constant of 5.0 ± 0.5 ms ($n = 20$). The mean latency of responses, calculated as a time interval between the end of the stimulation artifact and the beginning of the EPSC, was 2.6 ± 0.4 ms ($n = 20$). The EPSCs evoked by TN stimulations were completely blocked by the glutamate AMPA receptor antagonist CNQX (10 μM; $n = 5$) but were insensitive to the NMDA receptor blocker D-aminophosphonovalerate (D-AP5; 50 μM, $n = 5$, Fig. 3*B*).

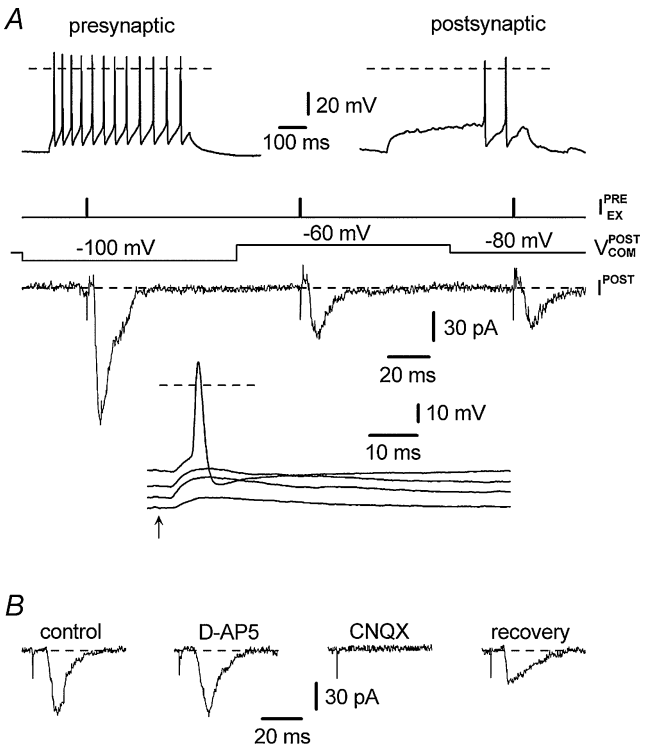

Figure 3. Connections of presynaptic TNs from the SG
A, examples of recordings obtained from one monosynaptic excitatory connection between a TN from the SG and a postsynaptic DN from the SG (25-day-old rat). Recorded EPSCs are given with the corresponding stimulation protocols (above). The current-clamp traces show EPSPs at different membrane potentials in a postsynaptic neuron. The time moment of a cell-attached stimulation of a presynaptic neuron is indicated by an arrow. Note that substantial membrane depolarization of postsynaptic DN was needed for EPSPs to reach the threshold of action potential firing. *B*, EPSCs in the control solution and in the presence of 10 μM CNQX and 50 μM D-aminophosphonovalerate (D-AP5).

The two inhibitory connections of TNs from the SG were interlaminar with a TN from lamina I and with a DN from lamina III (Fig. 6*A*, marked by asterisk).

Presynaptic ANs

All 17 presynaptic ANs were excitatory interneurons (Fig. 4*A*). In accordance with our previous results (Santos *et al.* 2004; Melnick *et al.* 2004*b*), they were mostly found in the lateral SG. In parasagittal sections, ANs were seen only if the surface of the slice included a part of the lateral SG (Fig. 6*B*). Of 17 presynaptic ANs, 12 formed intralaminar contacts with SG neurons (71%), three with lamina I neurons, and two had terminals in lamina III (Table 2). On the basis of firing patterns, presynaptic ANs formed contacts with 6 TNs, 1 AN and 10 DNs. All three excitatory connections to lamina I neurons recorded here were with TNs. The distances between coupled neurons varied from 9 to 54 μm, the mean distance being 21.1 ± 2.9 μm ($n = 17$).

The mean maximum EPSC amplitude was 103.3 ± 33.8 pA ($n = 15$) and the time constant of a decay was 5.0 ± 0.4 ms ($n = 15$). The mean latency was 2.6 ± 0.3 ms ($n = 15$). As with the presynaptic TNs, we also found that EPSCs associated with AN firing were completely blocked by 10 μM CNQX ($n = 4$) but not 50 μM D-AP5 ($n = 4$; Fig. 4*B*).

Excitatory DNs

Of 36 presynaptic DNs 23 were excitatory interneurons (Fig. 5*A*), and 74% of their connections ($n = 17$) were intralaminar with another SG neuron (Fig. 6*C*): 10 with TNs, 6 with ANs, and only 1 with a DN. Beyond the

Table 2. Connections of presynaptic SG neurons

	Postsynaptic neuron									
	Lamina I			Lamina II (SG)			Lamina III			
Presynaptic neuron (SG)	TN	AN	DN	TN	AN	DN	TN	AN	DN	Total
All connections ($n = 102$)										
TN	7 + 1*	—	—	21	8	7	2	—	2 + 1*	49
AN	3	—	—	3	1	8	—	—	2	17
DN (inhibitory)	7	—	—	2	—	3	—	—	1	13
DN (excitatory)	3	—	—	10	6	1	—	—	3	23
2 weeks ($n = 11$)										
TN	1	—	—	1	—	—	1	—	—	3
AN	1	—	—	2	—	—	—	—	—	3
DN (inhibitory)	2	—	—	1	—	—	—	—	—	3
DN (excitatory)	—	—	—	2	—	—	—	—	—	2
3 weeks ($n = 36$)										
TN	3 + 1*	—	—	15	4	2	1	—	1*	27
AN	1	—	—	—	1	2	—	—	—	4
DN (inhibitory)	—	—	—	—	—	2	—	—	—	2
DN (excitatory)	1	—	—	2	—	—	—	—	—	3
4–7 weeks ($n = 55$)										
TN	3	—	—	5	4	5	—	—	2	19
AN	1	—	—	1	—	6	—	—	2	10
DN (inhibitory)	5	—	—	1	—	1	—	—	1	8
DN (excitatory)	2	—	—	6	6	1	—	—	3	18

TN, tonic neuron; AN, adapting neuron; DN, delayed-firing neuron. The upper part of the table summarizes all connections obtained in this study. In lower parts of the table, the data are separated in three groups being presented for 2-week-old rats (postnatal days 15–20), 3-week-old rats (postnatal days 21–27) and 4- to 7-week-old rats (postnatal days 28–49). *Inhibitory connections of presynaptic TNs.

SG, DNs showed excitatory connections with three TNs in lamina I and 3 DNs in lamina III.

The mean value of maximum EPSC was 75.1 ± 16.8 pA ($n = 10$) at -100 mV, with a latency of 2.5 ± 0.4 ms ($n = 10$). The time constant of EPSC decay was 4.5 ± 0.5 ms ($n = 10$). We found that CNQX at 10 μM ($n = 7$), but not 50 μM D-AP5 ($n = 7$), completely blocked the EPSCs (Fig. 5*B*). The mean distance between coupled neurons was 23.8 ± 3.3 μm ($n = 23$; range from 6 to 59 μm).

Inhibitory DNs

The remaining 13 presynaptic DNs were identified as inhibitory interneurons (Fig. 7*A*). A majority of their postsynaptic connections were formed with lamina I neurons ($n = 7$), while only 38% ($n = 5$) with SG neurons (Fig. 7*C* and Table 2). A remaining connection was with another DN from lamina III. Thus, most connections of inhibitory DNs were interlaminar. All seven connections formed in lamina I were with TNs. In total, 13 DNs inhibited 9 TNs and 4 DNs. The distances between coupled neurons varied from 9 to 36 μm, and the mean distance was 21.6 ± 2.5 μm ($n = 13$).

The mean maximum IPSC amplitude was 75.8 ± 28.9 pA ($n = 10$) for inward currents at -100 mV, and 26.5 ± 3.3 pA ($n = 10$) for outward currents at -60 mV. The latency of the inhibitory synaptic response was 2.4 ± 0.4 ms ($n = 10$). The decay kinetics of the IPSCs were fast, the mean time constant was 5.3 ± 0.8 ms ($n = 11$) measured at -100 mV. These IPSCs were completely blocked by the glycine receptor antagonist strychnine (1 μM, $n = 6$, Fig. 7*B*), but not by picrotoxin (100 μM, $n = 5$, Fig. 7*B*).

Finally, we compared major parameters of inhibitory and excitatory DNs: R_{IN}, V_R, the current-clamp membrane time constant, the threshold of the action potential and the spike overshoot (Table 3). None of these parameters was found to be significantly different between two populations of DNs.

Control experiments

To test whether the low frequency of recording from inhibitory SG interneurons might be due to some limitations in the experimental protocol, we changed several parameters and specifically searched for inhibitory interneurons (for this reason the data were not included in the main statistics). First, although the slice thickness in

the above experiments was sufficient to preserve dendritic trees in most types of SG neurons (Grudt & Perl, 2002; Melnick *et al.* 2004*a*,*b*), we further increased the thickness to 500–600 μm in both parasagittal and transverse slices to ensure a complete preservation of distal dendrites. In these parasagittal sections, the slice thickness exceeded the mediolateral extensions of dendrites in all types of SG and lamina I neurons (Grudt & Perl, 2002). In transverse slices, the thickness exceeded the rostrocaudal dimensions of all SG neurons and nonprojection lamina I neurons (Grudt & Perl, 2002). Lamina I projection neurons, with the largest rostrocaudal dendritic extension (mean >700 μm), probably also preserved distal parts of dendrites remaining in the slice, if it was taken into consideration that any sectioning close to the soma of a superficial neuron unavoidably cut about a half of its dendritic tree and the other half is smaller than the thickness of our transverse slice. Second, we changed the amplitude of the first step in the testing voltage command to −120 mV to increase the driving force for IPSCs and therefore their resolution. Third, we made recordings from presumably not connected neuron pairs in 10 μM CNQX, to ensure that IPSCs in these pairs were not masked by glutamate-mediated EPSCs of the same magnitude, and finally we made recordings from pairs of neurons located in the centre of the SG near the interface of laminae II_i and II_o, where Lu & Perl (2003) found inhibitory GABAergic connections.

Under these conditions, we tested an additional 409 pairs of neurons: 107 in parasagittal and 302 in transverse slices. Only 24 neuron pairs (5.9%) were monosynaptically connected. Nineteen connections were excitatory and therefore were not subjected to further study. The remaining five connections were inhibitory. In three of them, the IPSCs were blocked by 1 μM strychnine but not by 100 μM picrotoxin, indicating a glycinergic nature of presynaptic neurons. One of these presynaptic neurons was a DN and two were TNs. In the two remaining connections, the IPSCs were completely blocked by addition of 100 μM picrotoxin but not by 1 μM strychnine. One of these GABAergic presynaptic neurons was a DN shown in Fig. 8, while the other was a TN (not shown). In both GABAergic neurons, the IPSCs were clearly seen at −120 and −60 mV (Fig. 8*A* and *B*) as well as at −100 mV (not shown). Both GABAergic neurons were found near the interface of lamina II_o and II_i, where a total of 54 neuron pairs were

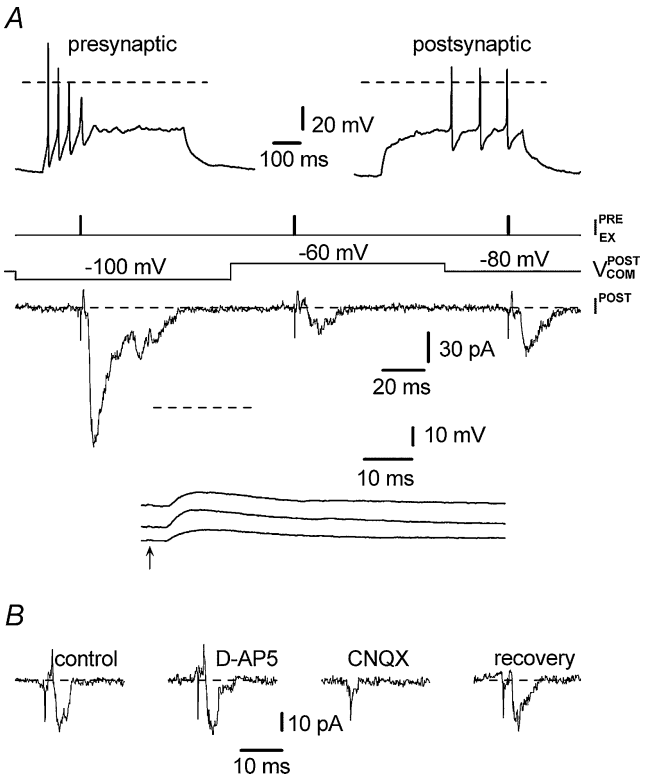

Figure 4. Excitatory connections of ANs
A, examples of recordings obtained from one connection between a presynaptic AN from the SG and a postsynaptic DN from lamina III (26-day-old rat). EPSCs and EPSPs at different voltages in the postsynaptic neuron. The time moment of a cell-attached stimulation of a presynaptic neuron in current-clamp traces is indicated by an arrow. *B*, EPSCs in control solution and in the presence of 10 μM CNQX and 50 μM D-AP5.

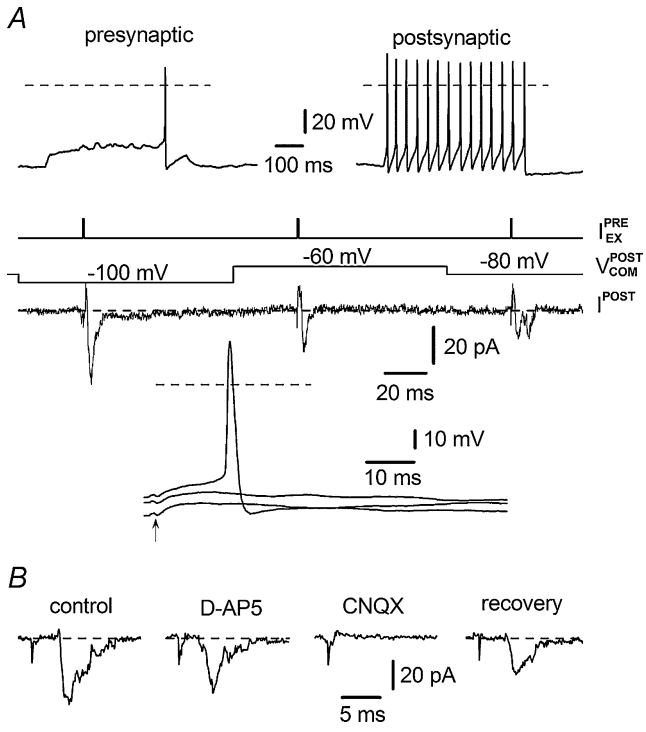

Figure 5. Monosynaptic excitatory connections of DNs
A, examples of recordings from a connection between a presynaptic DN from the SG and a postsynaptic TN from lamina I (26-day-old rat). EPSCs and EPSPs at different voltages were recorded in the postsynaptic neuron. The time moment of a cell-attached stimulation of a presynaptic neuron in current-clamp traces is indicated by an arrow. *B*, EPSCs in control solution and in the presence of 10 μM CNQX and 50 μM D-AP5.

tested. In eight pairs of apparently not connected neurons, recordings were also done in the presence of 10 μM CNQX. In none of them IPSCs became visible after addition of the blocker, indicating that in these pairs IPSCs were not masked by EPSCs.

Thus, these control experiments confirmed the adequate resolution of IPSCs in all our experiments and the overall low percentage of inhibitory connections of SG neurons with their possible region-specific localization.

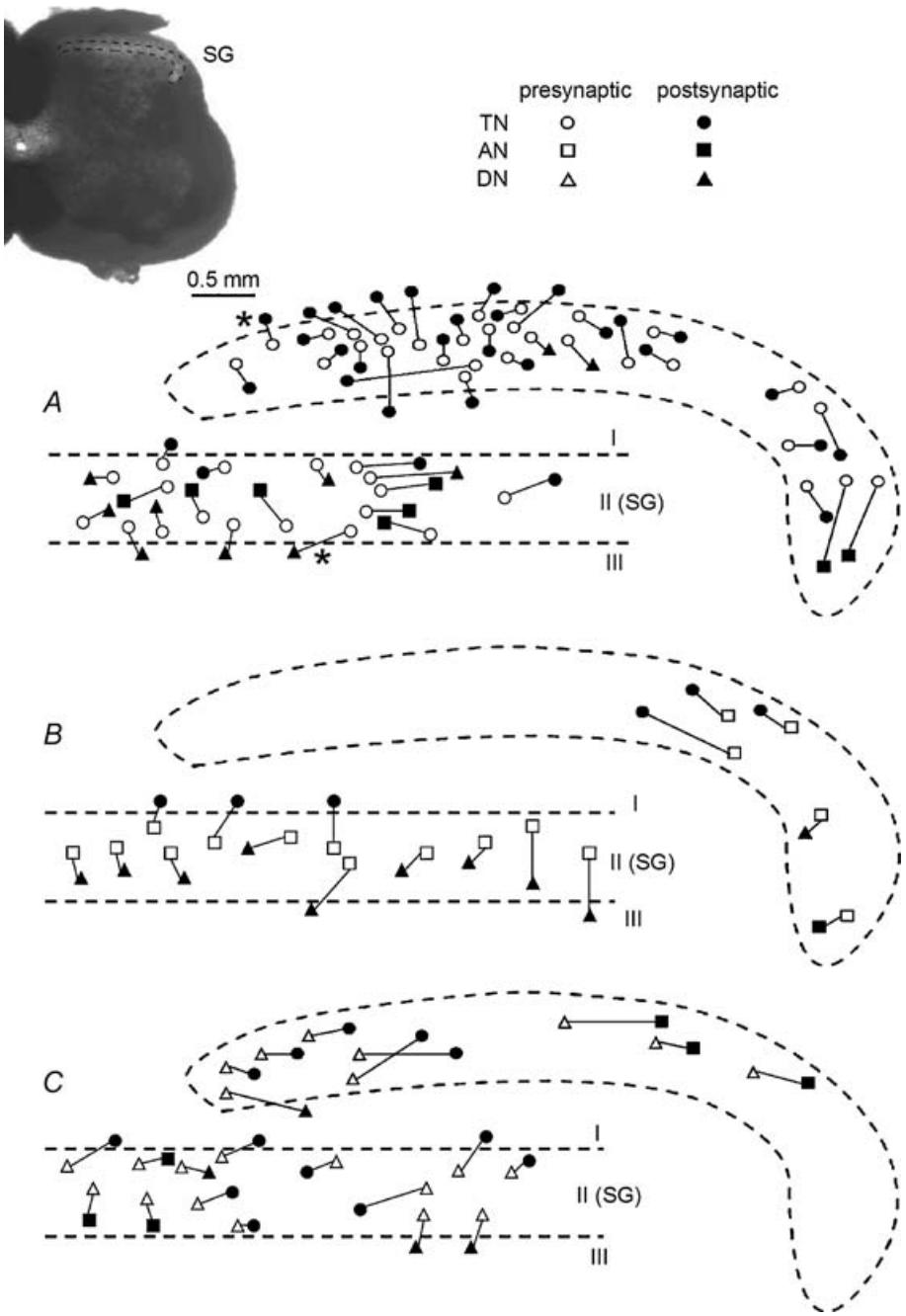

Figure 6. Distribution of excitatory connections of presynaptic SG interneurons
The diagrams of distributions of excitatory connections between presynaptic TNs (*A*), ANs (*B*) and DNs (*C*) from the SG and different types of postsynaptic neurons located in laminae I, II (SG) and III. Data from both transverse (upper) and parasagittal (lower) sections. Dashed lines indicate the border of the SG. In this and the following figure, all pre- and postsynaptic neurons are indicated by open and filled symbols, respectively. The two inhibitory connections of TNs are marked by asterisks in *A*.

Table 3. Comparison of inhibitory and excitatory DNs

	R_{IN}	V_R	Membrane time constant	Spike threshold	Spike overshoot	DN subtype			
	(GΩ)	(mV)	(ms)	(mV)	(mV)	DN_1	DN_2	DN_3	Total
Inhibitory	1.74 ± 0.43 (10)	-74.1 ± 0.7 (10)	64.3 ± 15.5 (10)	-45.7 ± 1.2 (10)	$+17.4 \pm 3.1$ (10)	8	3	2	13
Excitatory	1.72 ± 0.18 (10)	-73.4 ± 0.9 (10)	63.5 ± 7.19 (10)	-46.3 ± 1.6 (10)	$+11.6 \pm 1.6$ (10)	9	7	7	23
t Test	$P = 0.98$, n.s.	$P = 0.55$, n.s.	$P = 0.97$, n.s.	$P = 0.77$, n.s.	$P = 0.11$, n.s.	—	—	—	—

The parameters were compared by independent Student's *t* test, n.s., not significant. Description of minor differences between subtypes DN_1, DN_2 and DN_3 of DNs is given in Methods. Numbers of recordings are given in parentheses.

Discussion

The principal finding of this study is that the intrinsic integration in the SG is dominated by excitatory processing. We implemented a novel experimental strategy for efficiently identifying neuronal connections and found that 85% of axosomatic or axodendritic connections formed by SG interneurons were excitatory. Such a high proportion of excitatory interneurons is in a good agreement with previous morphological studies. *In situ* hybridization for three types of vesicular glutamate transporters VGLUT1, 2 and 3 revealed their expression in 38, 33 and 6% of laminae I–II neurons, respectively (Landry *et al.* 2004). Since 14% of neurons positive for either VGLUT1 or VGLUT2 were also positive for both these transporters, one can estimate that glutamatergic neurons represent 68% of the neuronal population. Another study found that 31 and 14% of SG neurons were GABA and glycine

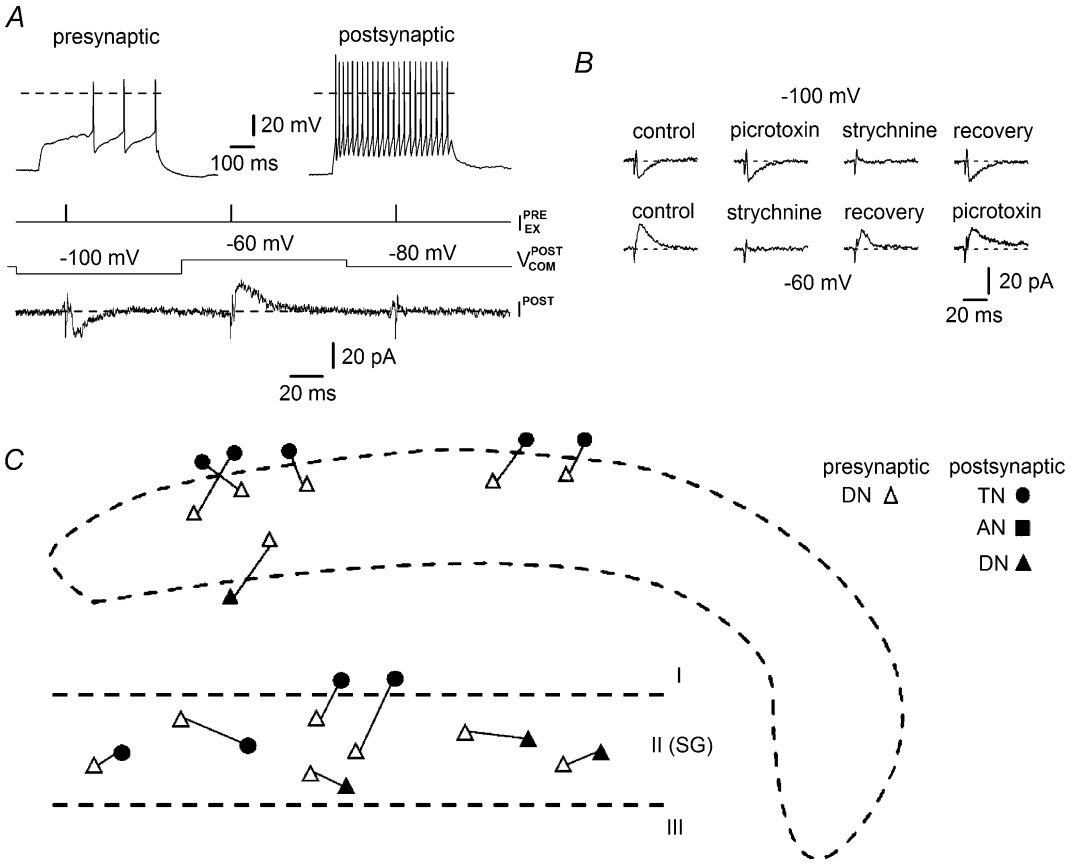

Figure 7. Monosynaptic connections of inhibitory DNs
A, recordings from an inhibitory connection between a presynaptic DN from the SG and a postsynaptic TN from the SG (19-day-old rat). IPSCs at different voltages in the postsynaptic neuron. *B*, IPSCs in control solution and in the presence of 1 μM strychnine or 100 μM picrotoxin. Recordings were made at −100 and −60 mV from the same neuron. *C*, the distributions of monosynaptic connections between inhibitory DNs from the SG and different postsynaptic neurons located in laminae I–III.

immunoreactive, respectively, and all glycine-immunoreactive cells were also GABA immunoreactive (Todd & Sullivan, 1990), suggesting that inhibitory interneurons represented 31% of SG neurons. These estimates for excitatory and inhibitory neurons are highly consistent with our data if one assumes that some inhibitory neurons may form presynaptic axoaxonic synapses and therefore cannot be detected by our technique. It is also possible that somata of excitatory interneurons originate a larger number of axonal collaterals and functional synapses than the somata of inhibitory interneurons.

In terms of integral organization of the SG neuronal network, our data suggest that, regardless of firing pattern, a majority of SG excitatory interneurons form intralaminar connections, while those of inhibitory SG neurons are mostly interlaminar. The relative number of inhibitory connections was higher for projections from the SG to lamina I (8 of 21, Table 2) and to lamina III (2 of 11, Table 2) being lower for internal projections within the SG (5 of 70, Table 2). The latter may indicate that spontaneous miniature IPSCs recorded in a vast majority of SG neurons (Chéry & De Koninck, 1999) are mostly induced by neurons located outside the SG.

We have also demonstrated that intrinsic firing of a SG neuron correlates with its function in such a way that a vast majority of TNs and ANs are excitatory interneurons, whereas DNs could be both excitatory and inhibitory interneurons. An adequate classification of neuronal firing patterns was critical for this study. Because of conflicting reports on discharge properties and membrane parameters of SG neurons, we took several precautions to ensure correct identification. In particular, we used the voltage-follower with a balanced input (Santos *et al.* 2004) to measure V_R and R_{IN}, studied passive membrane properties and discharge patterns at physiological temperatures and recorded through perforated patches to maximally preserve the intracellular environment critical for measured parameters. These experiments confirmed the three basic types of SG neurons, i.e. TNs, ANs and DNs, proposed previously (Grudt & Perl, 2002; Santos *et al.* 2004). Our whole-cell recordings have also shown that a BAPTA-based internal solution preserved the physiological firing patterns. This suggests that (1) these neurons have highly buffered Ca^{2+} under normal physiological conditions, and (2) firing patterns are highly Ca^{2+} dependent.

Our observations may also help to explain discrepancies in firing patterns between different reports. We found that the mean R_{IN} was above 1 GΩ and V_R was close to −70 mV for all cell types. High R_{IN} appears to be important for correct identification of TNs. Indeed, in the majority of them, the tonic firing could be selectively transformed into adapting upon R_{IN} reduction, for example, due to GIRK current activation by μ-opioids (Santos *et al.* 2004). Likewise, lowering R_{IN} in ANs frequently transformed their typical pattern into a single spike (unpublished observations). However, the basic firing pattern of both TNs and ANs was weakly sensitive to V_R, due to low expression of transient K^+ channels (Melnick *et al.* 2004*a*,*b*). In contrast, V_R was critical for correctly identifying DNs. Membrane depolarization can inactivate a pronounced transient K^+ current conductance and shorten the characteristic delay of the firing onset (Yoshimura & Jessell, 1989), thus inducing a tonic-like discharge. Furthermore, transient K^+ current in dorsal horn neurons was inhibited by Ca^{2+}-dependent protein kinase C and A (Hu & Gereau, 2003; Hu *et al.* 2003), suggesting that insufficient buffering for Ca^{2+} may transform the delayed-onset firing into tonic firing.

TNs in the SG can function as signal integrators (Prescott & De Koninck, 2002) because their discharge frequency increases with the stimulation intensity being regulated by the apamin-sensitive Ca^{2+}-activated K^+ conductance (Melnick *et al.* 2004*a*). Their axons project to the SG itself as well as to neighbouring laminae I and III (Melnick *et al.* 2004*a*). The present study shows that the vast majority of TNs are excitatory neurons interconnecting laminae I, II and III. The most abundant type of their connection was intralaminar with other

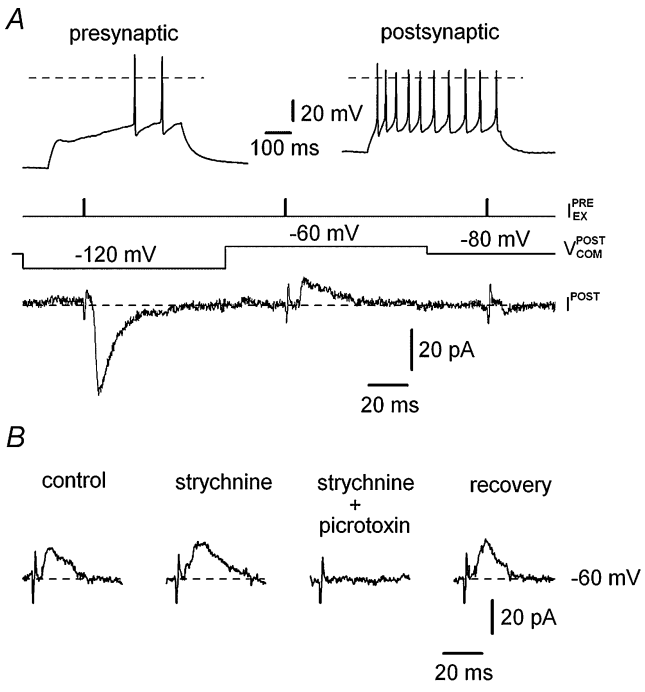

Figure 8. Monosynaptic connection of a GABAergic inhibitory DN

A, an inhibitory connection between a presynaptic DN and a postsynaptic TN in the SG (17-day-old rat). IPSCs recorded at −120, −60 and −80 mV in the postsynaptic neuron. *B*, IPSCs in control solution, in the presence of 1 μM strychnine and in the presence of 1 μM strychnine and 100 μM picrotoxin. At −60 mV, all recordings are from the same neuron.

TNs. This implies that excitatory circuitry involving two intrinsic TNs form an important block in SG processing. Importantly, excitatory TNs synapse on TNs from lamina I, a region where most nociceptive projection neurons are located (Burstein *et al.* 1987; Lima & Coimbra, 1988; Lima, 1998).

We have recently shown that TN is the only SG cell type directly inhibited by the μ-opioid agonist (Santos *et al.* 2004). The present classification of TNs as predominantly excitatory interneurons strongly supports the idea of specific targeting of postsynaptic μ-opioid receptors to excitatory SG interneurons (Kemp *et al.* 1996). Because of their numerous excitatory connections throughout the superficial dorsal horn, a selective inhibition of TNs may underlie the analgesic postsynaptic effects of endogenous enkephalins and administered opioids (Duggan *et al.* 1977; Johnston & Duggan, 1981).

ANs are preferentially located in the lateral SG and their dendritic tree and axonal arborization have pronounced rostrocaudal orientation, with a limited spread in the mediolateral and dorsoventral dimentions (Santos *et al.* 2004; Melnick *et al.* 2004*b*). Their characteristic firing adaptation results from a relatively low expression of voltage-gated Na^+ channels and is not regulated by Ca^{2+}-dependent K^+ mechanisms (Melnick *et al.* 2004*b*). The 'input–output' properties allow ANs to function as coincidence detectors (Prescott & De Koninck, 2002). Here we further show that ANs are excitatory interneurons forming most of their functional connections with local SG neurons. In the context of neuronal network therefore ANs appear to be mostly involved in the intralaminar excitatory processing within the lateral SG.

DNs can be both excitatory and inhibitory interneurons. Our statistical analysis did not reveal differences in membrane parameters between these two subpopulations. The majority of excitatory DNs made connections within the SG with local TNs. In contrast, inhibitory DNs formed most connections with lamina I TNs. Some of them released glycine acting on the strychnine-sensitive receptors. This is in accordance with observations that spontaneous miniature IPSCs in lamina I neurons were almost exclusively mediated through strychnine-sensitive glycine receptors (Chéry & De Koninck, 1999). The mean time constant of the IPSC decay (5.3 ms) obtained here is close to that of glycine-receptor-mediated IPSCs in lamina I–II neurons (Chéry & De Koninck, 1999). In general, membrane properties of DNs allow them to act as input integrators with a high firing threshold regulated by transient K^+ current. Modulation of transient K^+ current by protein kinase A and C, as well as by membrane potential, provides the mechanisms for the regulation of sensory processing in both excitatory and inhibitory circuitries.

The present data are in agreement with excitatory connections reported for ANs and DNs (Lu & Perl, 2005). According to our control experiments, a few per cent of TNs and DNs in the SG can also be GABAergic interneurons. Indeed, the GABAergic neurons with tonic firing were identified by simultaneous recordings (Lu & Perl, 2003) or green fluorescent protein expression (Hantman *et al.* 2004). It seems that neuron pairs with GABAergic connections are mostly localized in a narrow transitional zone between laminae II_i and II_o (Lu & Perl, 2003; our observations) and therefore the probability of finding them in the rest of the SG is very low. It is also possible that (1) in the majority of inhibitory synapses formed by SG neurons, $GABA_A$ receptors are extrasynaptic and therefore coreleased GABA and glycine predominantly evoke glycine-mediated IPSCs (Chery & De Koninck, 1999); and/or (2) some GABAergic neurons in the SG are involved in presynaptic inhibition of primary afferent terminals (reviewed in Lima, 1996), and thus cannot be identified by simultaneous recording from neuronal pairs.

One essential finding of this study is that excitatory synapses dominating the neuronal network in the SG are glutamatergic. Our results also indicate that fast synaptic transmission in these synapses is mediated through AMPA and/or kainate receptors, since EPSCs were completely blocked by CNQX. Although kainate receptors had been implicated in the synaptic transmission of Aδ- and C-fibre inputs to the SG (Youn & Randic, 2004) and in the modulation of transmitter release (Engelman & MacDermott, 2004), their activation under our experimental conditions was unlikely because it required much higher intensity of stimulation (Frerking *et al.* 1998; Lee *et al.* 2004), and EPSCs mediated by kainate receptors had much slower kinetics (Frerking *et al.* 1998; Cossart *et al.* 2002). In contrast, our data imply involvement of AMPA receptors, thus being consistent with observations of others that AMPA receptors are highly expressed in the superficial dorsal horn synapses (Tachibana *et al.* 1994; Tolle *et al.* 1995; Petralia *et al.* 1997) and modulate spinal synaptic plasticity and inflammatory pain (Hartmann *et al.* 2004).

In conclusion, the present study has revealed that the sensory integration in the SG is dominated by excitatory processing and that the intrinsic firing properties of SG interneurons correlate with their functions. Excitatory processing is mostly intralaminar, in contrast to the inhibition, which is preferentially interlaminar. This organization of neuronal circuitries in the spinal SG can be important for nociceptive encoding.

References

Bentley GN & Gent JP (1994). Electrophysiological properties of substantia gelatinosa neurones in a novel adult spinal slice preparation. *J Neurosci Methods* **53**, 157–162.

Brown AG (1981). *Organization in the Spinal Cord*. Springer-Verlag, Berlin, Heidelberg.

Burstein R, Cliffer KD & Giesler GJ Jr (1987). Direct somatosensory projections from the spinal cord to the hypothalamus and telencephalon. *J Neurosci* **7**, 4159–4164.

Cervero F (1987). Dorsal horn neurones and their sensory inputs. In *Spinal Afferent Processing*, ed.Yaksh TL, pp. 197–216. Plenum Press, New York.

Chéry N & De Koninck Y (1999). Junctional versus extrajunctional glycine and $GABA_A$ receptor-mediated IPSCs in identified lamina I neurons of the adult rat spinal cord. *J Neurosci* **19**, 7342–7355.

Cossart R, Epsztein J, Tyzio R, Becq H, Hirsch J, Ben-Ari Y & Crepel V (2002). Quantal release of glutamate generates pure kainate and mixed AMPA/kainate EPSCs in hippocampal neurons. *Neuron* **35**, 147–159.

Duggan AW, Hall JG & Headley PM (1977). Suppression of transmission of nociceptive impulses by morphine: selective effects of morphine administered in the region of the substantia gelatinosa. *Br J Pharmacol* **61**, 65–76.

Engelman HS & MacDermott AB (2004). Presynaptic ionotropic receptors and control of transmitter release. *Nat Rev Neurosci* **5**, 135–145.

Frerking M, Malenka RC & Nicoll RA (1998). Synaptic activation of kainate receptors on hippocampal interneurons. *Nat Neurosci* **1**, 479–486.

Graham BA, Brichta AM & Callister RJ (2004). *In vivo* responses of mouse superficial dorsal horn neurones to both current injection and peripheral cutaneous stimulation. *J Physiol* **561**, 749–763.

Grudt TJ & Perl ER (2002). Correlations between neuronal morphology and electrophysiological features in the rodent superficial dorsal horn. *J Physiol* **540**, 189–207.

Hantman AW, van den Pol AN & Perl ER (2004). Morphological and physiological features of a set of spinal substantia gelatinosa neurons defined by green fluorescent protein expression. *J Neurosci* **24**, 836–842.

Hartmann B, Ahmadi S, Heppenstall PA, Lewin GR, Schott C, Borchardt T, Seeburg PH, Zeilhofer HU, Sprengel R & Kuner R (2004). The AMPA receptor subunits GluR-A and GluR-B reciprocally modulate spinal synaptic plasticity and inflammatory pain. *Neuron* **44**, 637–650.

Horn R & Marty A (1988). Muscarinic activation of ionic currents measured by a new whole-cell recording method. *J Gen Physiol* **92**, 145–159.

Hu H-J & Gereau RW (2003). ERK integrates PKA and PKC signaling in superficial dorsal horn neurons. II. Modulation of neuronal excitability. *J Neurophysiol* **90**, 1680–1688.

Hu H-J, Glauner KS & Gereau RW (2003). ERK integrates PKA and PKC signalling in superficial dorsal horn neurons. I. Modulation of A-type K^+ currents. *J Neurophysiol* **90**, 1671–1679.

Ji RR, Kohno T, Moore KA & Woolf CJ (2003). Central sensitization and LTP: do pain and memory share similar mechanisms? *Trends Neurosci* **26**, 696–705.

Johnston SM & Duggan AW (1981). Evidence that opiate receptors of the substantia gelatinosa contribute to the depression, by intravenous morphine, of the spinal transmission of impulses in unmyelinated afferents. *Brain Res* **207**, 223–228.

Kemp T, Spike RC, Watt C & Todd AJ (1996). The μ-opioid receptor (MOR1) is mainly restricted to neurons that do not contain GABA or glycine in the superficial dorsal horn of the rat spinal cord. *Neurosci* **75**, 1231–1238.

LaMotte C (1977). Distribution of the tract of lissauer and the dorsal root fibers in the primate spinal cord. *J Comp Neurol* **172**, 529–561.

Landry M, Bouali-Benazzouz R, El Mestikawy S, Ravassard P & Nagy F (2004). Expression of vesicular glutamate transporters in rat lumbar spinal cord, with a note on dorsal root ganglia. *J Comp Neurol* **468**, 380–394.

Lee CJ, Labrakakis C, Joseph DJ & Macdermott AB (2004). Functional similarities and differences of AMPA and kainate receptors expressed by cultured rat sensory neurons. *Neuroscience* **129**, 35–48.

Light AR & Perl ER (1977). Differential termination of large-diameter and small-diameter primary afferent fibers in the spinal dorsal gray matter as indicated by labelling with horseradish peroxidase. *Neurosci Lett* **6**, 59–63.

Lima D (1996). Endogenous pain modulatory system in the light of the gate control theory. *Pain Forum* **5**, 31–39.

Lima D (1998). Anatomical basis for the dynamic processing of nociceptive input. *Eur J Pain* **2**, 195–202.

Lima D & Coimbra A (1988). The spinothalamic system of the rat: structural types of retrogradely labelled neurons in the marginal zone (lamina I). *Neurosci* **27**, 215–230.

Lisman J & Spruston N (2005). Postsynaptic depolarization requirements for LTP and LTD: a critique of spike timing-dependent plasticity. *Nat Neurosci* **8**, 839–841.

Lopez-Garcia JA & King AE (1994). Membrane properties of physiologically classified rat dorsal horn neurons *in vitro*: correlation with cutaneous sensory afferent input. *Eur J Neurosci* **6**, 998–1007.

Lu Y & Perl ER (2003). A specific inhibitory pathway between substantia gelatinosa neurons receiving direct C-fiber input. *J Neurosci* **23**, 8752–8758.

Lu Y & Perl ER (2005). Modular organization of excitatory circuits between neurons of the spinal superficial dorsal horn (laminae I and II). *J Neurosci* **25**, 3900–3907.

Malenka RC & Bear MF (2004). LTP and LTD: an embarrassment of riches. *Neuron* **44**, 5–21.

Malenka RC & Nicoll RA (1999). Long-term potentiation – a decade of progress? *Science* **285**, 1870–1874.

Melnick IV, Santos SFA & Safronov BV (2004*b*). Mechanism of spike frequency adaptation in substantia gelatinosa neurones of rat. *J Physiol* **559**, 383–395.

Melnick IV, Santos SFA, Szokol K, Szucs P & Safronov BV (2004*a*). Ionic basics of tonic firing in spinal substantia gelatinosa neurons of rat. *J Neurophysiol* **91**, 646–655.

Petralia RS, Wang YX, Mayat E & Wenthold RJ (1997). Glutamate receptor subunit 2-selective antibody shows a differential distribution of calcium-impermeable AMPA receptors among populations of neurons. *J Comp Neurol* **385**, 456–476.

Prescott SA & De Koninck Y (2002). Four cell types with distinctive membrane properties and morphologies in lamina I of the spinal dorsal horn of the adult rat. *J Physiol* **539**, 817–836.

Rae J, Cooper K, Gates P & Watsky M (1991). Low access resistance perforated patch recordings using amphotericin B. *J Neurosci Methods* **37**, 15–26.

Rethelyi M (1977). Preterminal and terminal axon arborizations in the substantia gelatinosa of cat's spinal cord. *J Comp Neurol* **172**, 511–521.

Ruscheweyh R & Sandkuhler J (2002). Lamina-specific membrane and discharge properties of rat spinal dorsal horn neurones *in vitro*. *J Physiol* **541**, 231–244.

Salter MW (2005). Cellular signalling pathways of spinal pain neuroplasticity as targets for analgesic development. *Curr Top Med Chem* **5**, 557–567.

Santos SFA, Melnick IV & Safronov BV (2004). Selective inhibition of tonic-firing neurons in substantia gelatinosa by μ-opioid agonist. *Anesthesiology* **101**, 1177–1183.

Sugiura Y, Lee CL & Perl ER (1986). Central projections of identified, unmyelinated (C) afferent fibers innervating mammalian skin. *Science* **234**, 358–361.

Tachibana M, Wenthold RJ, Morioka H & Petralia RS (1994). Light and electron microscopic immunocytochemical localization of AMPA-selective glutamate receptors in the rat spinal cord. *J Comp Neurol* **344**, 431–454.

Thomson AM, West DC & Headley PM (1989). Membrane characteristics and synaptic responsiveness of superficial dorsal horn neurons in a slice preparation of adult rat spinal cord. *Eur J Neurosci* **1**, 479–488.

Todd AJ & Sullivan AC (1990). Light microscope study of the coexistence of GABA-like and glycine-like immunoreactivities in the spinal cord of the rat. *J Comp Neurol* **296**, 496–505.

Tolle TR, Berthele A, Zieglgansberger W, Seeburg PH & Wisden W (1995). Flip and Flop variants of AMPA receptors in the rat lumbar spinal cord. *Eur J Neurosci* **7**, 1414–1419.

Turrigiano GG & Nelson SB (2004). Homeostatic plasticity in the developing nervous system. *Nat Rev Neurosci* **5**, 97–107.

Willis WD & Coggeshall RE (1991). *Sensory Mechanisms of the Spinal Cord*. Plenum Press, New York.

Woolf CJ & Salter MW (2000). Neuronal plasticity: increasing the gain in pain. *Science* **288**, 1765–1769.

Yoshimura M & Jessell TM (1989). Membrane properties of rat substantia gelatinosa neurons *in vitro*. *J Neurophysiol* **62**, 109–118.

Youn DH & Randic M (2004). Modulation of excitatory synaptic transmission in the spinal substantia gelatinosa of mice deficient in the kainate receptor GluR5 and/or GluR6 subunit. *J Physiol* **555**, 683–698.

Acknowledgements

We thank Drs Larry Trussell, John Williams and Ed McCleskey for insightful comments and discussions. The work was supported by the grant from the Portuguese Foundation for Science and Technology funded by POCTI2010 and FEDER (to B.V.S.), Medical Research Foundation grant (to V.A.D.) and NIH grant (to V.A.D. and Dr Thomas Soderling).